


## RESEARCH ARTICLE

# Elevated viscosities in a simulated moving bed for $\gamma$ -aminobutyric acid recovery

A. Schultze-Jena<sup>1,2</sup>  | M.A. Boon<sup>1</sup> | R.C. Vroon<sup>1</sup> | P.J.Th. Bussmann<sup>1</sup> |  
A.E.M. Janssen<sup>2</sup> | A. van der Padt<sup>2,3</sup>

<sup>1</sup>Food and Biobased Research, Wageningen University and Research, Wageningen, The Netherlands

<sup>2</sup>Food Process Engineering, Wageningen University and Research, Wageningen, The Netherlands

<sup>3</sup>FrieslandCampina, Amersfoort, The Netherlands

## Correspondence

Dr. Floor Boon, Bornse Weiland 9, 6708 WG Wageningen, The Netherlands.  
Email: floor.boon@wur.nl

Process streams of agro-food industries are often large and viscous. In order to fractionate such a stream the viscosity can be reduced by either a high temperature or dilution, the former is not an option in case of temperature sensitive components. Such streams are diluted prior to chromatographic fractionation, resulting in even larger volumes and high energy costs for sub-sequential water removal. The influence of feed viscosity on the performance of simulated moving bed chromatography has been investigated in a case study of the recovery of a  $\gamma$ -aminobutyric acid rich fraction from tomato serum. This work addresses the chromatographic system design, evaluates results from a pilot scale operation, and uses these to calculate the productivity and water use at elevated feed concentration. At the two higher feed viscosities (2.5 and 4 mPa·s) water use is lower and productivity higher, compared to the lowest feed viscosity (1 mPa·s). The behavior of the sugars for different feed viscosities can be described well by the model using the ratio of feed to eluent as dilution factor. The behavior of  $\gamma$ -aminobutyric acid is highly concentration dependent and the recovery could not be accurately predicted.

## KEYWORDS

chromatography, concentration profile, productivity, simulated moving bed, viscosity

## 1 | INTRODUCTION

Recovery of minor components from large agro-food streams offers a potential source for a variety of complex compounds. Due to the size of the available streams, these components are present in large quantities. Such components may be of value as functional ingredients in food products, however, they often are present in a mixture with less desired components (i.e., salts or mono- and disaccharides). For the food industry, such components are not only attractive with high purity, but

also in the form of enriched fractions and clean-label components [1]. This offers a window of opportunity to design recovery processes, which are restricted by food industry specific requirements. Those requirements generally stem from a combination of process economics and functionality of target components.

Non-destructive technologies are required, which leave the processed stream unspoiled from the (mild) separation process so that all fractions may remain useable. Economic aspects mandate that the technologies are scalable

Article Related Abbreviations: EC, electric conductivity; HFCS, high fructose corn syrup; RI, refractive Index; SMB, simulated moving bed.

This is an open access article under the terms of the Creative Commons Attribution-NonCommercial License, which permits use, distribution and reproduction in any medium, provided the original work is properly cited and is not used for commercial purposes.

© 2020 The Authors. *Journal of Separation Science* published by Wiley-VCH Verlag GmbH & Co. KGaA, Weinheim.

and energy efficient. Component functionality requires mild treatment throughout the process, avoiding harsh chemicals or high temperatures, preferring the use of water as process aid.

Chromatographic processes are technically well suited for these types of separations, since they target specific interactions between required compounds and stationary phase and are scalable [2]. In the pharmaceutical industry, chromatography is used to purify and fractionate complex molecules, such as proteins and peptides often on a relatively small scale. In the food industry, the examples are limited to large-scale applications such as high fructose corn syrup (HFCS) production and sucrose recovery from molasses [3]. Industrial-scaled preparative chromatography for food products could be done by using continuous multicolumn applications, like a simulated moving bed system with high productivities. Small and robust separation systems are required since they will use small amounts of rather expensive stationary phase, which is one of the main contributors to operation costs [4].

One way to reduce system size is the reduction of the feed volumetric flow rate. Feed streams can be reduced in volume by reduction of water content or by minimizing dilution of concentrated serums, syrups, extracts, and so on prior to the chromatographic separation. Generally, as the feed stream concentration decreases with dilution, resistance to mass transfer and pressure drop will decrease. With dilution feed stream volume increases. In this tradeoff between feed stream size and mass transfer resistance, column volume increases at highly diluted feed streams in single column operations [5].

This research investigates the impact of feed stream concentration on the productivity and water use in a simulated moving bed (SMB). The phenomena were studied using the case of obtaining an enriched  $\gamma$ -aminobutyric acid fraction from tomato serum using ion-exclusion chromatography. Tomato serum is produced from tomatoes through a series of mild processing steps, including solid removal and concentration and is used in food products to provide a fruity, fresh, sweetish-sour tomato flavor.  $\gamma$ -Aminobutyric acid is a small amino acid and of interest as an additive in food products, to promote mental health [6, 7] and reduce blood pressure [8]. In the scenario laid out in this study,  $\gamma$ -aminobutyric acid is separated from the saccharides present in the serum.

## 2 | MATERIALS AND METHODS

### 2.1 | Materials

#### 2.1.1 | Tomato serum

Tomato serum was supplied by Unilever, the Netherlands. The serum was supplied in cooled containers at a concen-

tration of 70°Bx and a viscosity of 271 mPa·s (measured at 20°C). The composition of tomato serum, as supplied by the manufacturer, is detailed in Supporting Information Table A1. The serum was diluted with Milli-Q water to reach concentrations of 7, 25, and 35°Bx, which amounts to 1, 2.5, and 4 mPa·s, respectively. For isotherm measurements, a model feed was used, as a defined and simplified version of the complex tomato serum.

#### 2.1.2 | Stationary phase

*Dowex 50WX4*, a cation exchange resin, was used as stationary phase. The mean particle diameter (106  $\mu\text{m}$ ) was measured with a Mastersizer 2000 (Malvern, UK). For the isotherm measurements and *SMB* pilot experiments, the stationary phase was equilibrated with an ion solution resembling the cationic composition of tomato serum: 38.35 g/L KCl, 3.28 g/L  $\text{CaCl}_2 \cdot 2\text{H}_2\text{O}$ , and 8.11 g/L  $\text{MgCl}_2 \cdot 6\text{H}_2\text{O}$ .

#### 2.1.3 | Chromatographic equipment

For single column measurements a Welchrom setup with a K-1001 gradient HPLC pump, combined with a dynamic mixer and injection valve, was used. Detection was done using a K-2600 UV detector and a CM 2.1S conductivity detector; all from Knauer, Germany. Additional detection was performed through a RI-502 RI detector from Shodex, Japan. Furthermore, a F25 MP water-bath (Julabo, Germany) was used to control the temperature in the column jacket and a mini Cori-Flow flowmeter (Bronkhorst, The Netherlands) was used to measure the flow rate after the detector. Elution profiles were measured in a Götec Superformance 300-10 column (300  $\times$  10 mm), packed to a bed height of 26.8 cm at a superficial velocity of 1.11 m/h.

The *SMB* pilot setup was built from six slurry packed Götec Superformance 300-16 columns (300  $\times$  16 mm) with tefzel capillaries of 35 cm length and ID 0.5 mm, including flow adapter with frits and filter (all Götec, Germany). The columns were connected in series in a 2/1/2/1 configuration, with 26.6 cm average bed height, and 53.4 mL average bed volume. Water jackets of all columns were connected in line with a F25 MP water bath (Julabo, Germany) to control the column temperature at 20°C. Four pumps, two for delivery of eluent (Milli-Q water) and feed (tomato serum) and two for extraction of raffinate and extract flows, were used, all up to 50 mL/min (Knauer, Germany). One pump (250 mL/min) was used for recycling eluent from *SMB* section 4 to section 1 (Knauer, Germany). Five multi-position valves (Knauer, Germany) were used for distribution of inlets (eluent and feed) and outlets (raffinate, extract, and recycle) over the *SMB* columns.

The *SMB* was inline monitored at the extract and raffinate outlets using refractive index K-2401 RI detectors (Knauer, Germany) and conductivity (GE Healthcare, USA) detectors,

respectively. Pump flows were monitored with inline mini CORI-FLOW flow meters (Bronkhorst, The Netherlands) at the pump outlets. Temperature of two column outlets was measured with inline thermocouples.

## 2.2 | Methods

### 2.2.1 | Column characterization

In preparation of the SMB pilot experiments, six columns were packed and characterized by pulse experiments. Prior to column packing, the resin was conditioned with a K/Ca/Mg solution, to avoid swelling or shrinking of the stationary phase during operation. Columns were packed in Milli-Q, followed by bed compression with a 4 mPa·s sugar solution at 15 mL/min (450 cm/h). Next, the columns were characterized by measuring bed height, porosities (bed and total porosity), and distribution coefficients of target components (glucose and minerals). It was shown that all columns were uniformly packed, by comparing pulse elution profiles, bed porosities, and distribution coefficients.

### 2.2.2 | Isotherm measurement

The linear isotherms of fructose and glucose were determined from pulse injections. The nonlinear isotherm of  $\gamma$ -aminobutyric acid had to be measured via a different method and was determined from frontal analysis of breakthrough times as described in [9]. All isotherm measurements were carried out in mobile phase of three viscosities: 1, 4, and 12.5 mPa·s, corresponding to 7, 35, and 50°Bx tomato serum, respectively. To increase viscosity fructose, glucose, and sucrose were used in the same ratio as in tomato serum (35% total sugars for 4 mPa·s and 51% total sugars for 12.5 mPa·s).

### 2.2.3 | Chromatographic analysis

The lumped kinetic model was used to describe mass transfer (equation 1), based on ref. [10].

$$\text{HETP} = \frac{2D_L}{u_L} + \frac{2u_L}{k_{\text{overall}} \cdot \frac{1-\varepsilon_b}{\varepsilon_b}} \cdot \left( \frac{k_1}{1+k_1} \right)^2 \quad (1)$$

HETP (m) is the height equivalent to a theoretical plate, measured from pulse experiments as described in ref. [11].  $D_L$  is the axial diffusion coefficient ( $\text{m}^2/\text{s}$ ) in the mobile phase, which combines longitudinal diffusion and eddy dispersion in the moving eluent [12],  $u_L$  is the interstitial linear velocity (m/s),  $k_{\text{overall}}$  the lumped kinetic factor (1/s),  $\varepsilon_b$  bed porosity (–), and  $k_1$  the zone retention factor (–).

From the slopes of the linear part of van Deemter curves, in HETP (m) over interstitial linear velocity  $u_L$  (m/s), the lumped

kinetic factor  $k_{\text{overall}}$  (1/s) was calculated with equation (2) [13].

$$k_{\text{overall}} = \frac{\frac{2}{\frac{1-\varepsilon_b}{\varepsilon_b}} \cdot \left( \frac{k_1}{1+k_1} \right)^2}{\left( \frac{\text{HETP}}{u_L} \right)} \quad (2)$$

The zone retention factor  $k_1$  calculated from equation (3), with the particle porosity  $\varepsilon_p$  and the slope of the isotherm  $\frac{\partial q}{\partial c}$ , based on ref. [10].

$$k_1 = \frac{1-\varepsilon_b}{\varepsilon_b} \left( \varepsilon_p + (1-\varepsilon_p) \frac{\partial q}{\partial c} \right) \quad (3)$$

Intraparticle diffusivity  $D_p$  ( $\text{m}^2/\text{s}$ ) was then calculated from equation (4) [13].

$$D_p = \frac{r_p^2}{15 \left( \frac{1}{k_{\text{overall}}} - \frac{r_p}{3 \cdot k_{\text{film}}} \right)} \quad (4)$$

With  $r_p$  particle radius (m) and the resistance to mass transfer through the stagnant film layer  $k_{\text{film}}$  (m/s), calculated as a function of reduced velocity  $\nu = (2 \times r_p \times u_L)/D_m$  (–) from the correlation of Wilson and Geankoplis [14] as shown in equation (5).

$$k_{\text{film}} = \frac{1.09}{\varepsilon_b} \frac{D_m}{2 \times r_p} \nu^{1/3} \quad (5)$$

## 2.3 | Viscosity measurement

Mobile phase viscosity was measured with a Physica MCR 301 rheometer (Anton Paar, Austria) at 20°C.

## 2.4 | SMB design

A SMB design model was used based on the lumped kinetic model. Six columns were distributed over the four sections of the SMB in a 2/1/2/1 configuration. First, an initial estimate of flows, size of the columns, and switch time, was obtained from the triangle theory [15] was used. In a second step the design was optimized in *gProms Modelbuilder 5.1.1*. dynamic optimization routine, by finding ideal velocities for each section. The optimization objective was the maximization of feed flow over water input and the constrains were a 95% removal of sugar and  $\gamma$ -aminobutyric acid recovery of 99%. In these design calculations and to facilitate evaluation of practical results, the same pressured drop in the system for all viscosities was maintained (4 bar per column). All concentrations were calculated after 15 cycles of the entire system, well into steady state operation.  $\gamma$ -Aminobutyric acid recovery was calculated with equation (6), from mineral concentration in the raffinate  $c_{\text{mineral, raff}}$  ( $\text{kg}/\text{m}^3$ ), raffinate flow rate

$q_{\text{raff}}$  (m<sup>3</sup>/h), feed concentration  $c_{\text{mineral.feed}}$  (kg/m<sup>3</sup>), and feed flow rate  $q_{\text{feed}}$  (m<sup>3</sup>/h).

$$\text{Recovery}_{\gamma\text{-aminobutyric acid}} = \frac{c_{\text{mineral.raff}} \times q_{\text{raff}}}{c_{\text{mineral.feed}} \times q_{\text{feed}}} \times 100\% \quad (6)$$

Sugar removal was calculated with equation (7), from summed glucose and fructose concentration in the extract  $c_{\text{sugar.extr}}$  (kg/m<sup>3</sup>), extract flow rate  $q_{\text{extr}}$  (m<sup>3</sup>/h), summed glucose and fructose concentration in the raffinate  $c_{\text{sugar.raff}}$  (kg/m<sup>3</sup>), and raffinate flow rate  $q_{\text{raff}}$  (m<sup>3</sup>/h).

$$\begin{aligned} \text{Removal}_{\text{sugars}} &= \frac{c_{\text{sugar.extr}} \times q_{\text{extr}}}{c_{\text{sugar.extr}}} \times q_{\text{extr}} + c_{\text{sugar.raff}} \\ &\times q_{\text{raff}} \times 100\% \end{aligned} \quad (7)$$

Productivity was calculated from equation (8) with feed concentration of  $\gamma$ -aminobutyric acid  $c_{\gamma\text{-aminobutyric acid.feed}}$  (kg/m<sup>3</sup>), the recovery of  $\gamma$ -aminobutyric acid (-), the feed flow rate  $q_{\text{feed}}$  (m<sup>3</sup>/h), and the system volume  $V_{\text{SMB}}$  (volume of six columns, m<sup>3</sup>).

$$\text{Productivity} = \frac{c_{\gamma\text{-aminobutyric acid.feed}} \times \text{Recovery}_{\gamma\text{-aminobutyric acid}} \times q_{\text{feed}}}{V_{\text{SMB}}} \quad (8)$$

Water use was calculated as the sum of eluent (water input) and water required for feed dilution. Water required for feed dilution was calculated with equation (9) from the feed stream  $q_{\text{feed}}$  (m<sup>3</sup>/h) and dilution factor  $DF$  (-).

$$\text{Water for dilution} = q_{\text{feed}} - \frac{q_{\text{feed}}}{DF} \quad (9)$$

With dilution factors of 10, 2.2, and 2, concentrated tomato serum (70°Bx) was diluted to viscosities of 1, 2.5, and 4 mPa·s, respectively.

## 2.5 | SMB operation

For each feed viscosity three experiments were performed in which the switch time was adjusted. For 1 mPa·s (7°Bx) the switch times were 1.25, 1.38, and 1.44 min, for 2.5 mPa·s (25°Bx) the switch times were 1.57, 1.72, and 1.80 min, and for 4 mPa·s (35°Bx) the switch times were 2.00, 2.20, and 2.30 min. All flows were kept constant. For each feed viscosity, the optimal switch time calculated was the lowest switch time. During the start-up of each experimental series, the flows were adapted in such a way that the pressure drop in the first section was approximately 4 bar.

## 2.6 | Viscosity estimation

The viscosity was estimated as an average over the system by using the ratio of feed and eluent (water) as dilution factor. The so estimated viscosity was compared to the viscosity calculated from the measured pressure drop. The pressure drop was measured with two EZG10 pressure sensors (Knauer, Germany) over one column which changed position with each column switch. During steady state operation, the viscosity in the system was estimated via the average pressure drop, using the Ergun equation (equation [10]), with pressure drop  $\Delta p$  (Pa), column length  $L$  (m), mobile phase viscosity  $\mu_{\text{bulk}}$  (Pa·s), particle diameter  $d_p$  (m), bed porosity  $\varepsilon_b$  (-), mobile phase density  $\rho$  (kg/m<sup>3</sup>), and superficial linear velocity  $u_S$  (m/s) [16].

$$\Delta p = \frac{150\mu_{\text{bulk}}}{d_p^2 L} \frac{(1 - \varepsilon_b)^2}{\varepsilon_b^3} u_S + \frac{1.75\rho}{d_p L} \frac{(1 - \varepsilon_b)}{\varepsilon_b^3} u_S^2 \quad (10)$$

The total sugar concentration within each column was also analyzed at the end of experiments for each feed viscosity.

## 3 | RESULTS AND DISCUSSION

### 3.1 | Simulated moving bed - design

Tomato serum was analyzed for its key components (Supporting Information Table A1). The elution profile of each key component was recorded from pulse injections, an overlay of all elution profiles, recorded via the refractive index (RI), is given in Figure 1a. The profiles of the saccharides and  $\gamma$ -aminobutyric acid were well separated, the later showed little to no retention, eluting together with the minerals. Figure 1b shows the same pulse injections as Figure 1a, with an overlay of diluted (1:10) tomato serum. The profile of tomato serum was recorded via RI and electric conductivity (EC). The (RI) overlay showed that the key components of the complex tomato serum are well represented by the individually injected components. The EC overlay showed that almost all charged components are in the first peak. These charged components had almost no retention and were thus excluded from the intraparticle pore volume. Based on these results it was decided, for practical reasons, to use minerals as an indicator for  $\gamma$ -aminobutyric acid during the design.

The viscosity of the tomato serum differed from the viscosity of the pure fructose and/or glucose mixtures. Figure 2

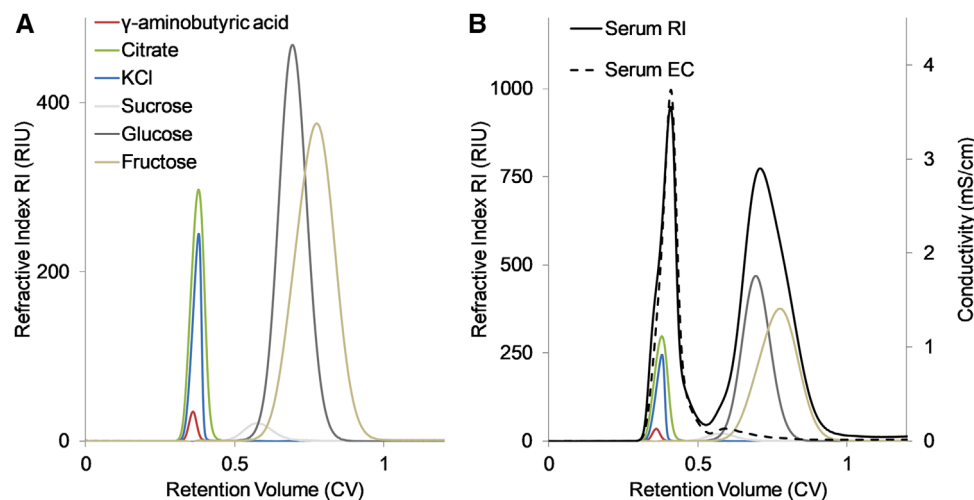


**FIGURE 1** (A) Overlay of eluted peaks from pulse injections of the key components of tomato serum detected via RI. (B) Overlay of the same key components but with the additional overlay of diluted tomato serum detected with RI and EC

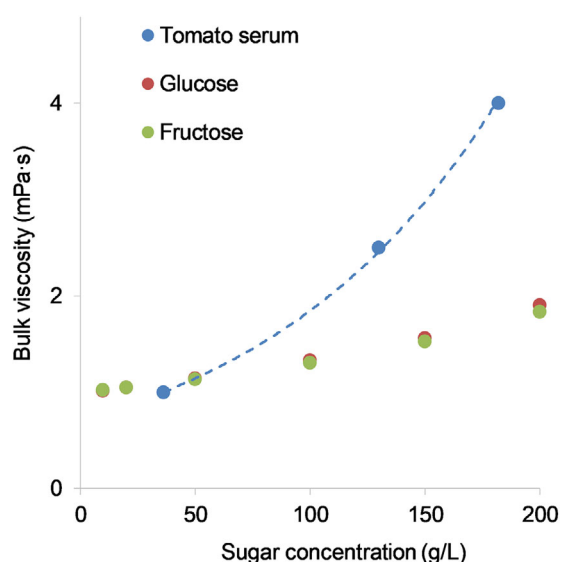


**FIGURE 2** Difference in viscosity between tomato serum, glucose, and sucrose solutions at equivalent concentrations

shows the viscosity measured in tomato serum as a function of total sugar concentration (sum of fructose and glucose). The viscosity was much larger than data based on literature for either monosaccharide [17]. This is an indication for the presence of an, so far, unidentified molecule that influences viscosity. This unknown contribution to viscosity, made the description of concentration and viscosity profiles inside the SMB system inaccurate, as we will show later.

The SMB process was designed to fractionate the feed stream into an enriched  $\gamma$ -aminobutyric acid fraction (low affinity, raffinate port) and saccharide fraction (high affinity, extract port). To establish the equilibria of the separation, the isotherms were measured for the two major saccharide components (glucose and fructose) and minerals (as indicator for

**TABLE 1** Kinetic parameters calculated for the different viscosities

		Viscosity [mPa·s]		
		1	2.5	4
$k'_{\text{overall}}$ [1/s]	Fructose	0.30	0.19	0.16
	Glucose	0.30	0.19	0.16
	$\gamma$ -Aminobutyric acid	0.23	0.10	0.07
$D_L$ [ $10^{-7}$ m <sup>2</sup> /s]	Fructose	6.96	2.80	1.75
	Glucose	6.96	2.80	1.75
	$\gamma$ -Aminobutyric acid	6.20	2.09	1.17

$\gamma$ -aminobutyric acid) as function of feed viscosities (1, 2.5, and 4 mPa·s). The affinity of fructose was slightly higher than of glucose, and with increasing viscosity, the affinity of both saccharides increased and was linear in the range measured. The minerals isotherm was convex, and showed no discernable dependence on viscosity. Both isotherms can be found in the Supporting Information (Figures A1 and A2, respectively). One mineral isotherm was fitted over the whole concentration range and for the three measured viscosities (black dashed line in Supporting Information Figure A2). Due to the convex isotherm of the minerals, the selectivity between the sugars and minerals (as indicator for  $\gamma$ -aminobutyric acid) decreased at increased tomato serum concentration, which made the separation more difficult.

Based on the isotherms, the flow rates in the different sections were calculated with the triangle theory [15] for each viscosity. With the estimated flow rates and the kinetic parameters given in Table 1, flow rates and switching times were optimized, in order to maximize productivity and minimize water input. Flow rates, switching times, and calculated recovery and sugar removal are listed in Supporting Information Table A2.



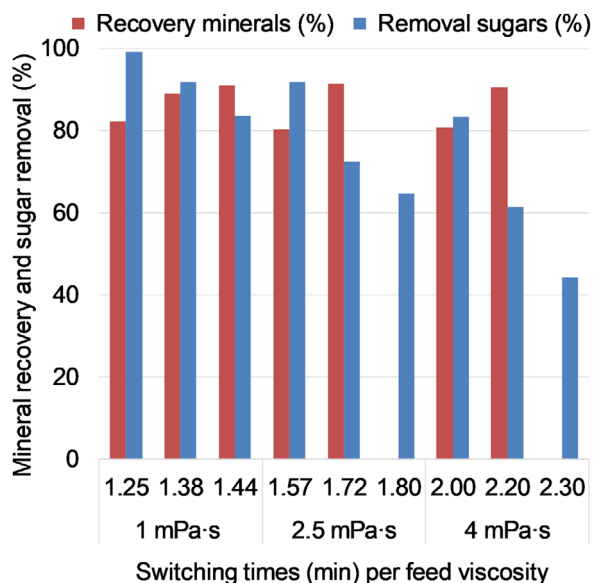


**FIGURE 3**  $\gamma$ -Aminobutyric acid recovery and saccharide removal for three different viscosities measured from pilot scale experiments. Switching times were increased twice within each experimental series. No data for  $\gamma$ -aminobutyric acid recovery at the longest switching time in 2.5 and 4 mPa·s

### 3.2 | Pilot results

Laboratory results often require slight adjustments of switching times from the calculated optima, a lesson learned through practical experience. Therefore, the experiments were repeated twice for each viscosity, each time increasing the switching time by approximately 25% (Supporting Information Table A2). For both process criteria, the saccharide removal and  $\gamma$ -aminobutyric acid recovery, and for all three switching times, the experimental results are shown in Figure 3. For the third switching time at viscosities of 2.5 and 4 mPa·s,  $\gamma$ -aminobutyric acid recovery was not measured. The figure shows that the recovery of  $\gamma$ -aminobutyric acid was dependent on the feed viscosity, the results varying from about 55% (1 mPa·s, switch time 1) to about 80% (4 mPa·s, switch time 2). The removal of sugar was decreasing at higher feed viscosities. Further, the trade-off between  $\gamma$ -aminobutyric acid recovery and sugar removal is visible. With increasing switch time the sugar removal decreases as the  $\gamma$ -aminobutyric acid recovery increases.

The separation process resulted in enriched fractions of  $\gamma$ -aminobutyric acid. However, neither the target concentration of  $\gamma$ -aminobutyric acid, nor the targeted sugar removal reached the levels the process was designed for. With the exception of sugar removal at 1 mPa·s (switch time 1), none of the values fell in the calculated range. To find an explanation for the discrepancy between the measured values and model, the distribution of viscosity within the system was analyzed.

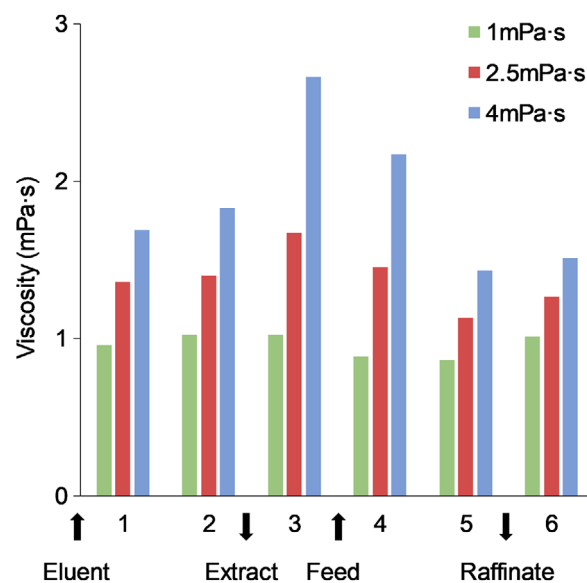


**FIGURE 4** Viscosity for each column within the system and the feed viscosities of 1, 2.5, and 4 mPa·s. For orientation, the ports of eluent, extract, feed, and raffinate are marked between the columns

### 3.3 | Viscosity distribution inside the simulated moving bed

In the SMB design a constant viscosity, equal to the feed concentration, was assumed. Figure 4 shows the viscosity profile, measured via pressure drop, for each column in the SMB. At low viscosities (1 mPa·s), the effect of dilution was not visible. However, at higher feed viscosity (2.5 and 4 mPa·s), dilution was observed and viscosity clearly varied between the columns. Figure 4 shows good agreement with the expected relative distribution of viscosity throughout the system: the highest viscosities were measured in columns 3 and 4, downstream and upstream of the feed port, respectively. Moreover, Figure 4 also shows that for feed with elevated viscosity, nowhere in the system viscosities as high as the feed viscosity were measured, even at the highest viscosity in column three, the measured viscosity was about two-thirds of the feed viscosity (1.7 mPa·s for 2.5 mPa·s feed and 2.7 mPa·s for 4 mPa·s feed). In the model input for the design of the pilot experiments, all parameters were based on the isotherm and mass transfer kinetics measurements at the feed viscosity. In the multicolumn separation, the input feed was diluted with the desorbent stream (water) and this should be taken into account.

Since the viscosity was reduced by dilution with water, the ratio of feed to eluent flow rate was used as dilution factor to estimate the average viscosity inside the SMB system. From the dilution factor the total sugar concentration was calculated (given in Table 2). The total sugar concentration in grams per liter is proportional to °Bx. From the plot of viscosity as function of sugar concentration, the viscosity of the diluted feed was fitted (Supporting Information Figure A3). The estimated

**TABLE 2** Average viscosities within the SMB system, as measured via pressure drop and estimated from dilution, based on ratio of eluent over feed flow. All viscosities in (mPa·s)

Feed viscosity (mPa·s)	1.0	2.5	4
Average viscosity measured via pressure drop (mPa·s)	1.0	1.4	1.9
Ratio of flowrate eluent over feed ( $q_{\text{eluent}}/q_{\text{feed}}$ ) (-)	2.2	2.5	2.4
Total sugar concentration after dilution (g/kg)	16.0	53.0	76.0
Average viscosity based on dilution (mPa·s)	1.0	1.2	1.5

**TABLE 3** Kinetic parameters calculated for the different viscosities based on dilution of feed stream

		Feed viscosity [mPa·s]		
		1	2.5	4
Average viscosity based on dilution [mPa·s]		1.0	1.2	1.5
$k'_{\text{overall}}$ [1/s]	Fructose	0.30	0.28	0.26
	Glucose	0.30	0.28	0.26
	$\gamma$ -Aminobutyric acid	0.23	0.21	0.18
$D_L$ [ $10^{-7}$ m <sup>2</sup> /s]	Fructose	6.96	6.31	5.31
	Glucose	6.96	6.31	5.31
	$\gamma$ -Aminobutyric acid	6.20	5.55	4.56

viscosities were 1.2 and 1.5 mPa·s for 2.5 and 4 mPa·s feed, respectively. These were slightly lower than the measured values via pressure drop (1.4 and 1.9 mPa·s, respectively). The isotherms (Supporting Information Figure A4) and mass transfer parameters (Table 3) were re-evaluated for these average viscosities based on concentration. The isotherm for the minerals (as indicator for  $\gamma$ -aminobutyric acid) was independent of viscosity and was not changed (Supporting Information Figure A2). The change in mass transfer kinetics  $k'_{\text{overall}}$  and axial diffusivity  $D_L$  were also estimated based on viscosity (Table 3). Using these re-evaluated equilibrium and kinetic parameters, the performances of the pilot experiments were calculated in the model.

Figure 5a shows the comparison of laboratory pilot measurements versus model calculations, which were based on equilibrium and kinetic parameters determined for a constant viscosity, equal to the feed viscosity, in the SMB system. It is clear, that only the pilot data of sugar removal for 1 mPa·s feed concentration match the calculation; sugar removal at higher viscosities and all  $\gamma$ -aminobutyric acid recoveries showed poor agreement. The  $\gamma$ -aminobutyric acid recovery was always calculated to be close to 100%, independent of viscosity and switching time.

Figure 5b shows the calculation with the re-evaluated model parameters using the average viscosity based on

the feed and eluent viscosity. The model calculations were repeated. The calculation of 1 mPa·s feed concentration was the same. For both greater feed concentrations, it became apparent, that the calculated sugar removal was much closer to experimental values, even though the model overestimated sugar removal by roughly 10%. The change in saccharide removal could be attributed to the change in isotherms, the influence of the changed kinetic parameters was small. Also the influence of switching time is well represented in the model. The calculation of  $\gamma$ -aminobutyric acid recovery still requires improvement. It appears that the elution behavior of the mineral fraction is sensitive to concentration profiles within the system. In Figure 2, it was shown that viscosities of tomato serum and model solution were not in agreement, possibly due to an unknown molecule. The change in viscosity and its influence on thermodynamics and kinetics needs to be identified and understood.

Literature described that mineral isotherms are dependent on sugar concentration [18]. At greater sugar concentration, the capacity of the cation exchange resin for the minerals decreased. This could explain why a lower  $\gamma$ -aminobutyric acid recovery was observed at higher feed viscosities. Furthermore, during the pilot experiments, it was observed that divalent cations present in the tomato serum (such as Ca and Mg) were exchanged with the ions on the cation exchange resin (such as Na and K). It is known that the affinity of sugars for the cation exchange resin depends on the counter ion, and this may further have reflected on the mineral isotherms [19].

Additionally, viscous fingering, an instability at the interfaces between viscous sample and eluent, may have influenced the separation, at the two larger viscosities (2.5 and 4 mPa·s). The result of viscous fingering is an instable interface, leading to distorted peaks and therefore reduced separation performance [20]. It occurs where a low viscous liquid displaces a high viscous liquid. In the SMB operated at higher feed viscosities, this happens where the eluent enters the system and it therefore should have little influence on the recovery of  $\gamma$ -aminobutyric acid.

### 3.4 | Water use and productivity as function of feed input viscosity

The use of water and the productivity of the chromatographic system for different input stream viscosities were compared to evaluate the water saving potential and resin volume reduction of chromatography operated at higher viscosities. The comparison was made for optimized systems, minimal water input for eluent and maximum productivity, using the re-evaluated parameters for the average viscosity within the SMB. As the model overestimated  $\gamma$ -aminobutyric acid recovery compared to measurements in the pilot system, the results may be

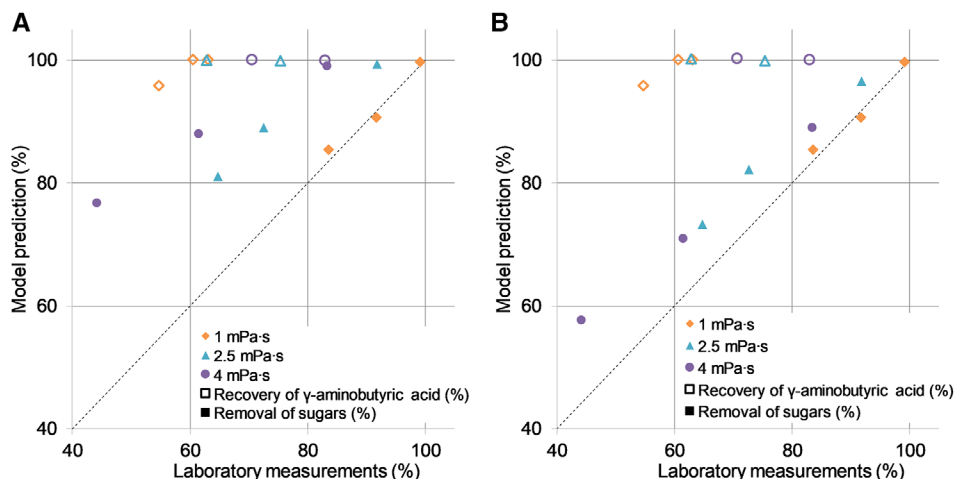


**FIGURE 5** Plot comparing model calculation to experimental results from the laboratory pilot system for  $\gamma$ -aminobutyric acid recovery and saccharide removal for three different viscosities and three switching times, (A) input parameters based on feed viscosity, (B) input parameter based on viscosity of feed diluted by eluent

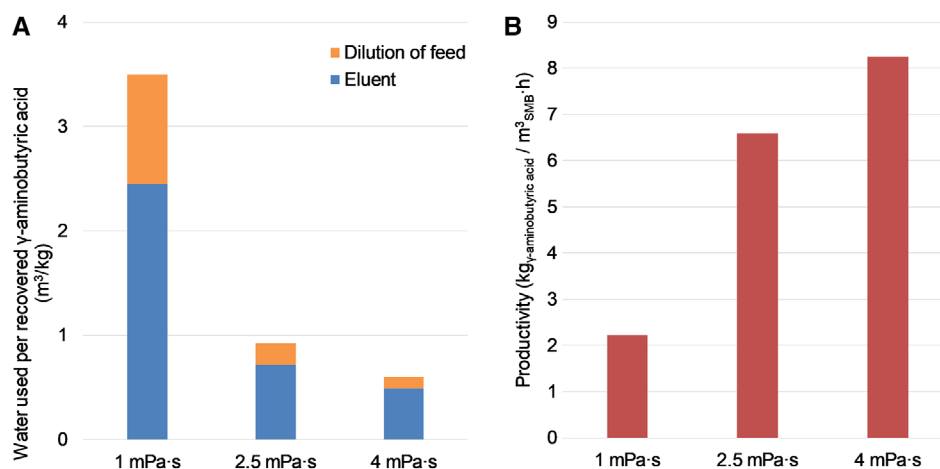


**FIGURE 6** After optimization of velocities in each section of the SMB, (A) water use per kilogram of recovered  $\gamma$ -aminobutyric acid for three feed viscosities for dilution of feed and for eluent use and (B) productivity for three feed viscosities were calculated

optimistic, but still serve the purpose of comparison. Water use for dilution of the concentrated tomato serum to the viscosities of the input stream was included in the total water use.

The recovered mass of  $\gamma$ -aminobutyric acid, by lieu of recovered mineral fraction, was compared to the use of water for eluent and feed dilution calculated in the model (Figure 6a). The comparison clearly showed that operating at higher viscosities (2.5–4 mPa-s) used much less water per kilogram of recovered target fraction and resulted in a higher productivity (mass of recovered product per system volume and time, Figure 6b). This result matched previously calculated column performances in single column experiments, where it was found that the trade-off between mass transfer and stream volume that was made when changing viscosity, lead to an increase in column volume in feed streams with viscosities below about 2.5 mPa-s.

## 4 | CONCLUSIONS

The footprint of an SMB system can be improved, by optimizing feed stream viscosity. Whether dilute streams are concentrated, or concentrated streams are diluted, a distinct change in productivity and water use is found in between viscosities of 1 and 2.5 mPa-s, the higher viscosity outperforming lower viscosity. Productivity is increased by a factor of around 3 and water use is reduced by around the same factor. The difference between 2.5 and 4 mPa-s is less pronounced, both in terms of productivity and water use. Within an SMB operated at higher feed concentrations, concentration dependent parameters can be estimated based on the dilution of the feed with the eluent. In this manner, the measured removal of sugars from tomato serum using ion-exclusion chromatography matches design calculations well. The measured recovery of  $\gamma$ -aminobutyric acid enriched fraction is not in agreement



with the model design. The behavior of  $\gamma$ -aminobutyric acid in such a system is very sensitive to concentration differences due to convex isotherms, sugar affinities that depend on the counter ion, and the interaction between the saccharides and the minerals, requiring the measurements of multi-component isotherms.

## ACKNOWLEDGMENTS

This research took place within the framework of the Institute for Sustainable Process Technology (ISPT). The authors would like to thank the ISPT for their support, together with Unilever (Vlaardingen, the Netherlands), FrieslandCampina Research (Amersfoort, the Netherlands), DSM (Delft, the Netherlands), and Cosun Food Technology (Roosendaal, the Netherlands) for their financial support and interest in this project.

## CONFLICT OF INTEREST

The authors have declared no conflict of interest.

## ORCID

A. Schultze-Jena  <https://orcid.org/0000-0001-9896-3881>

## REFERENCES

- Goot, A. J. v. d., Pelgrom, P. J. M., Berghout, J. A. M., Geerts, M. E. J., Jankowiak, L., Hardt, N. A., Keijer, J., Schutyser, M. A. I., Nikiforidis, C. V., Boom, R. M., Concepts for further sustainable production of foods. *J. Food Eng.* 2016, 168, 42–51.
- Schmidt-Traub, H., Schulte, M., Seidel-Morgenstern, A., Preparative Chromatography. 2nd ed., Wiley-VCH, Weinheim 2012.
- <https://www.dow.com/webapps/include/GetDoc.aspx?filepath=liquidseps/pdfs/noreg/177-03529.pdf> (cited 2019 August 01).
- Verzele, M., Industrial application of preparative liquid chromatography. *TrAC, Trends Anal. Chem.* 1987, 6, 202–205.
- Schultze-Jena, A., Boon, M. A., Vroon, R. C., Bussmann, P. J. T., Janssen, A. E. M., Padt, A. v. d., High viscosity preparative chromatography for food applications. *Sep. Purif. Technol.* 2020, 237, 116386.
- Jessen, K. R., Mirsky, R., Dennison, M. E., Burnstock, G., GABA may be a neurotransmitter in the vertebrate peripheral nervous system. *Nature* 1979, 281, 71–74.
- Kalueff, A. V., Nutt, D. J., Role of GABA in anxiety and depression. *Depression Anxiety* 2007, 24, 495–517.

- Ma, P., Li, T., Ji, F., Wang, H., Pang, J., Effect of GABA on blood pressure and blood dynamics of anesthetic rats. *Int. J. Clin. Exp. Med.* 2015, 8, 14296–14302.
- Vente, J. A., Bosch, H., Haan, A. B. d., Bussmann, P. J. T., Evaluation of sugar sorption isotherm measurement by frontal analysis under industrial processing conditions. *J. Chromatogr. A* 2005, 1066, 71–79.
- Felinger, A., Guiochon, G., Comparison of the kinetic models of linear chromatography. *Chromatographia* 2004, 60, 175–180.
- Schultze-Jena, A., Boon, M. A., Bussmann, P. J. T., Janssen, A. E. M., Padt, A. v. d., The counterintuitive role of extra-column volume in the determination of column efficiency and scaling of chromatographic processes. *J. Chromatogr. A* 2017, 1493, 49–56.
- Gritti, F., Guiochon, G., Mass transfer kinetics, band broadening and column efficiency. *J. Chromatogr. A* 2012, 1221, 2–40.
- Coquebert de Neuville, B., Tarafder, A., Morbidelli, M., Distributed pore model for bio-molecule chromatography. *J. Chromatogr. A* 2013, 1298, 26–34.
- Wilson, E. J., Geankoplis, C. J., Liquid mass transfer at very low Reynolds numbers in packed beds. *Ind. Eng. Chem. Fundam.* 1966, 5, 9–14.
- Carta, G., Jungbauer, A., Protein Chromatography. 1st ed., Wiley-VCH, Weinheim 2010.
- Ergun, S., Orning, A. A., Fluid flow through randomly packed columns and fluidized beds. *Ind. Eng. Chem.* 1949, 41, 1179–1184.
- <https://www.nordicsugar.com> (cited 2019 August 01).
- Lameloise, M.-L., Lewandowski, R., Purification of beet molasses by ion-exclusion chromatography: fixed-bed modelling. *J. Chromatogr. A* 1994, 685, 45–52.
- Vente, J., Bosch, H., Haan, A. B. d., Bussmann, P., Comparison of sorption isotherms of mono- and disaccharides relevant to oligosaccharide separations for Na, K, and Ca loaded cation exchange resins. *Chem. Eng. Commun.* 2005, 192, 23–33.
- Catchpole, H. J., Andrew Shalliker, R., Dennis, G. R., Guiochon, G., Visualising the onset of viscous fingering in chromatography columns. *J. Chromatogr. A* 2006, 1117, 137–145.

## SUPPORTING INFORMATION

Additional supporting information may be found online in the Supporting Information section at the end of the article.

**How to cite this article:** Schultze-Jena A, Boon MA, Vroon RC, Bussmann PJTh, Janssen AEM, van der Padt A. Elevated viscosities in a simulated moving bed for  $\gamma$ -aminobutyric acid recovery. *J Sep Sci.* 2020;1–9. <https://doi.org/10.1002/jssc.201900785>